International Journal of Mass Spectrometry and Ion Processes, 112 (1992) 1–17
Elsevier Science Publishers B.V., Amsterdam

Discrimination effects for ions with high initial kinetic energy in a Nier-type ion source and partial and total electron ionization cross-sections of CF_4

H.U. Poll[1], C. Winkler, D. Margreiter, V. Grill and T.D. Märk
Institut für Ionenphysik, Leopold Franzens Universität, Technikerstrasse 25, A 6020 Innsbruck (Austria)
(First received 26 October 1990; in final form 16 September 1991)

ABSTRACT

Fragment ions produced by dissociative electron impact ionization of molecules often have large amounts of kinetic energy (up to several electronvolts). Presently performed computer simulations of the ion trajectories in a Nier-type ion source show strong discrimination effects in the extraction characteristics of such ions, leading to huge errors in measured fragmentation patterns and absolute partial ionization cross-section functions. Using the simulation results a correction function (extraction efficiency vs. fragment kinetic energy) is calculated here for a given potential distribution of a Nier-type ion source extraction system. This correction procedure is applied to previously measured partial ionization cross-sections of CF_4. The corrected partial and total CF_4 cross-sections are in excellent agreement with other recent measurements using advanced methods.

Keywords: cross-section; discrimination effect; carbon tetrafluoride; ion-trajectory calculations.

INTRODUCTION

The quantitative determination of electron impact ionization cross-sections for atoms and molecules is a fundamental task in atomic physics, because of its importance for understanding the mechanism of electron impact ionization and because of the need for these cross-sections in applied physics, e.g. in plasma physics or mass spectrometry [1]. Besides the total ionization cross-section, the most important piece of information necessary for the detailed understanding of the ionization processes in a plasma or mass spectrometer ion source is a quantitative knowledge of partial ionization cross-sections.

Owing to great experimental difficulties (i.e. discrimination of energetic fragment ions in the ion source and mass spectrometer) only a small number of experiments exist in the literature reporting partial ionization cross-section functions of molecules [2]. Despite experimental shortcomings, but as a result

[1] Permanent address: Sektion Physik/Elektronische Bauelemente, Technische Universität, DO 9010 Chemnitz, Germany.

0168-1176/92/$05.00

TABLE 1

Overall composition of the ions produced by electron impact ionization of various molecules containing fluorine and/or chlorine according to measurements of partial ionization cross-sections [4–8]

Target molecule	Composition of all ions produced	Ref.
CF_4	$CF_{2.8}$	6, 7
C_2F_4	$C_2F_{3.0}$	7
C_2F_6	$C_2F_{5.1}$	7
C_3F_8	$C_3F_{7.7}$	7
C_4F_8	$C_4F_{7.3}$	5
C_4F_{10}	$C_4F_{9.5}$	7
CCl_4	$CCl_{2.7}$	8
CCl_2F_2	$CCl_{1.0}F_{1.6}$	8
SF_6	$SF_{3.9}$	4

of the great interest in plasma technology and low pressure plasma processing [3], several measurements were recently made concerning fluorine and chlorine compounds [4–8]. A comparison of the stoichiometry of the neutral parent molecules and of the stoichiometry of the total ion current produced by electron ionization (see Table 1), however, shows in all of these cases a significant deficit of small constituents in the ionized state, e.g. for CF_4 the sum of the produced ions (weighted with the respective partial ionization cross-sections) has a composition of $CF_{2.8}$. This fact may have several causes. Firstly, during the dissociative ionization process the charge might be preferentially retained by the larger fragments (e.g. for CF_4 a CF_n^+ fragment ion with $n < 4$) leading to too small a number of fluorine ions in the ionized state compared with the expectation value considering the stoichiometry. The second reason contributing to this effect is discrimination of energetic fragment ions during their extraction from the ion source and flight through the mass spectrometer. Owing to the Franck–Condon principle and the mechanism of dissociative ionization, fragment ions (in particular the smaller ones) are usually produced with excess kinetic energy. For instance, dissociative ionization of H_2 yields protons with energies peaking at around 8 eV [9]. Moreover, fragment ions resulting from the dissociative ionization of more complex polyatomic molecules, for instance hydrocarbons, also exhibit considerable excess kinetic energies [10–12]. This rather large kinetic energy of fragment ions leads to considerable discrimination effects in ordinary ion sources where the ions are extracted by rather weak electric fields through rather small slits [13].

The focal properties of ion sources have been studied by several authors in order to obtain information on the operating conditions and to determine

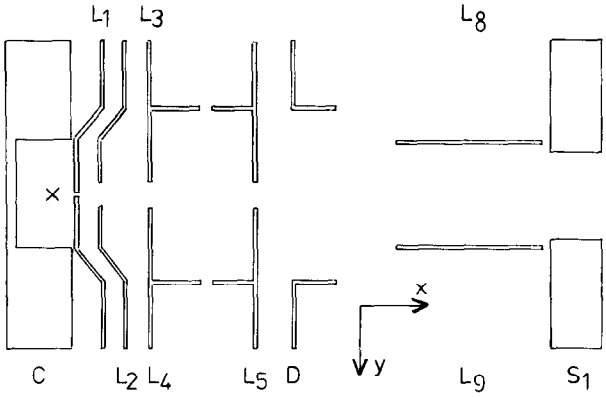

Fig. 1. Schematic (and simplified) view of the Nier-type ion source and the extraction and focussing system of a Varian MAT CH5 DF double focussing mass spectrometer, used for the computer simulation. C, collision chamber; L_1, collision chamber exit electrodes; L_2 and $L_{3,4}$, ion extraction and focussing electrodes; L_5, earth slit; D, defining aperture; $L_{6,7}$, z deflection plates perpendicular to $L_{8,9}$ (not shown); $L_{8,9}$, y deflection plates; S_1, mass spectrometer entrance slit; cross, position of electron beam with electrons moving in z direction.

mechanisms limiting source efficiency (see a review of this subject given in ref. 13). Most of the studies, however, are limited to thermal ions and to Nier-type ion sources using repeller voltage scans. Recently, it has been shown by Stephan et al. [14] that the performance of the Nier-type ion source can be considerably improved—at least for thermal ions—using a penetrating field extraction mode rather than repeller voltage scans. As an extension of all the previous work we have studied here the extraction of energetic ions from a Nier-type ion source operated in the penetrating field extraction mode. The results include calculated discrimination factors as a function of kinetic energy (correction function). This correction function may be used to correct measured partial ionization cross-sections yielding thereby rather accurate cross-section values. This will be demonstrated using CF_4 as a test case.

ION TRAJECTORIES AND KINETIC ENERGY CORRECTION FUNCTION

Geometry of the ion source

The present investigations are based on the geometry of the ion source and analyzer system of the double focussing mass spectrometer Varian MAT CH5DF as described in detail in refs. 14 and 15. Figure 1 shows a schematic (and simplified) view of the Nier-type ion source and the extraction and focussing system between ion source and mass spectrometer entrance slit S_1. The source and extraction system consists of a collision chamber C, an exit electrode L_1, extraction electrode L_2, focussing electrodes L_3 and L_4, earth slit

L_5 followed by a defining slit D, beam centring and deflection electrodes L_6–L_9 (L_6 and L_7, which are perpendicular to L_8 and L_9, are not shown in Fig. 1) and the mass spectrometer entrance slit S_1. Ions are produced by an electron beam, which is guided by a weak magnetic field. The electrons move parallel to the slit in L_1 at a distance of ≈ 3 mm from L_1 (see Fig. 1). The produced ions are extracted by a penetrating field (generated by L_2) and the ion beam ensuing from the accelerating region may be scanned across the mass spectrometer entrance slit S_1 in the z and y directions with the help of $L_{6,7}$ and $L_{8,9}$ respectively. Integration over these z and y ion beam profiles (see ref. 8) allows one to avoid discrimination effects at S_1. The gas to be studied may be introduced in this source either as a stagnant gas target or as a molecular beam (coming from a supersonic nozzle) crossing the electron beam perpendicular to the x–y plane in the y direction.

Method of calculation

The electrical potential and field distribution in the x–y plane and the respective ion trajectories have been calculated using the computer program SIMION [16] on an ordinary personal computer. The program was used in its plane geometry version with a spatial resolution of 0.5 mm and in the standard accuracy mode.

Electrical potential distribution (x–y plane)

Figure 2 gives as an example the electric potential distribution in the extraction region for typical experimental parameters. A voltage of $U = 3$ kV on C and L_1 with respect to the ground potential at L_5 serves in the experiment as the acceleration voltage of the ions. For simplicity we have used in the computer simulation ground potential on C and L_1 and -3 kV at L_5. The influence of the extraction electrode L_2, giving a potential energy of about 0.2 eV at the starting point of the ions inside the chamber (see also refs. 14 and 17), is clearly seen as well as the focussing properties of the lens system owing to strongly bent potential curves near the slits.

Ion trajectories (x–y plane)

Using the computer program SIMION it is also possible to calculate ion trajectories (under fixed electrical potential conditions) as a function of initial starting position, angle and kinetic energy of the ions. Assuming a fixed starting position at the crossing point of the electron beam and molecular beam, calculations show that ion trajectories with starting angles (with respect to the ion beam axis) larger than a specific maximum angle ϑ_{max} are being lost

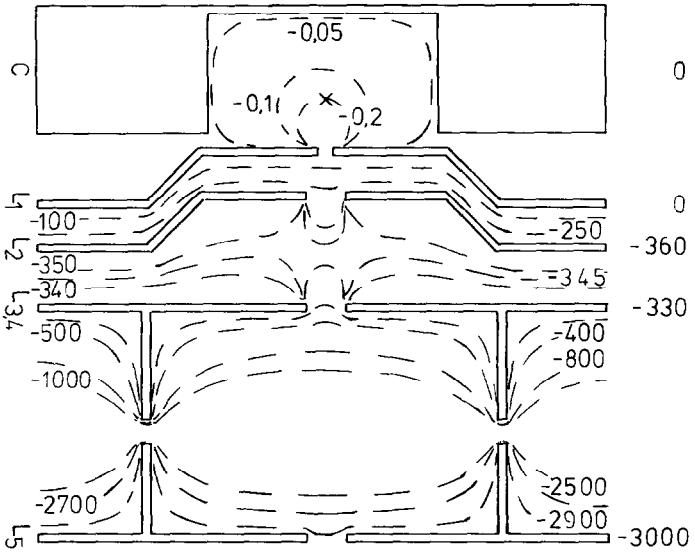

Fig. 2. Electrical potential distribution in the extraction and focussing region of the Nier-type ion source (Fig. 1) under typical experimental conditions. All values are given in volts.

at one of the electrodes (in particular L_1 and to a much lesser degree at $L_{3,4}$). It turns out that the maximum angle is strongly dependent upon the initial kinetic energy. Moreover, it is interesting to note that under experimental extraction and focussing conditions as shown in Fig. 2 thermal ions (with energies of several tens of millielectronvolts) are already subject to discrimination, the calculated maximum angle for these thermal ions being $\vartheta_{max} = \pm 67°$. In the case of ions with a starting energy of 1 eV the maximum angle is only $\pm 12°$. This is illustrated in detail in Fig. 3. It is interesting to note that almost all ions with angles larger than ϑ_{max} are lost at L_1, whereas only

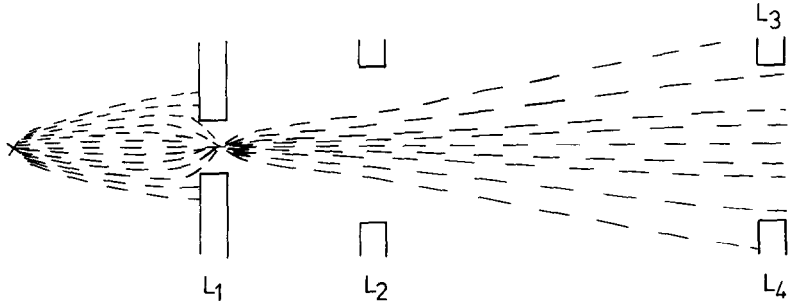

Fig. 3. Ion trajectories in the extraction region of the Nier-type ion source (Fig. 1) for ions with an initial energy of 1 eV. The figure shows the trajectories exemplarily with starting angles close to or smaller than the maximum starting angle ϑ_{max} (see text).

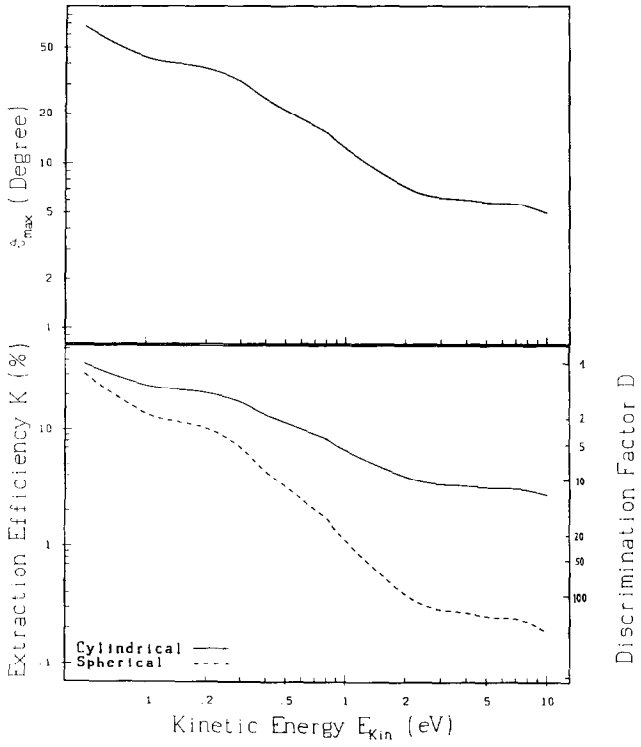

Fig. 4. (a; top) Maximum starting angle ϑ_{max} vs. kinetic energy of the ion. (b; bottom) Extraction efficiency K (left-hand scale) and discrimination factor D (right-hand scale) vs. kinetic energy of the ion assuming different geometries of the ion source. For definition of K and D see text.

a few ions are lost downstream at L_3 and L_4. This indicates that the chosen operating conditions lead to a rather ideal flight path through the focussing electrodes of this system (see also below) once the ions have left the source exit.

Correction function

Figure 4a shows the calculated maximum angle ϑ_{max} as a function of the kinetic energy E_{kin} ($0 < E_{kin} < 10\,eV$) for the usual ion source operating conditions. The dependence of ϑ_{max} on E_{kin} is strongest in the energy region between thermal and $\approx 2\,eV$. This is of particular interest, because fragment ions usually have energies in this range. This obviously leads to rather large differences in extraction efficiency for fragment ions of different kinetic energies in this energy region. It is clear that without correction measured fragment ion abundances and ratios are meaningless. Almost all previous measurements of this kind (e.g. mass spectral fragmentation patterns) do not

take into account this large energy dependent discrimination effect (see the discussion in the introduction).

In order to correct measured ion abundances and ratios (which serve as the basis for partial cross-section determinations) it is necessary to define an extraction efficiency $K = K(E_{kin})$, with K being the ratio between extracted ions and ions generated in the ion source. Assuming slits (see Fig. 1) of infinite length in the z direction (amounting to a cylindrical symmetry) K is given by

$$K = \vartheta_{max}/180° \tag{1}$$

it follows that for example only 37% of the thermal ions and only 6.8% of ions with 1 eV kinetic energy will be extracted. The extraction efficiency is even smaller assuming spherical symmetry (that is if the slit lengths in the z direction were of the same order as the slit widths) where K is given by

$$K = \sin^2(\vartheta_{max}/2) \tag{2}$$

In this case K decreases to 30.5% for thermal ions and to 1.1% for ions with 1 eV. In this context it is interesting to point out that extraction geometries approximated by this relation (for instance hole apertures in quadrupole mass spectrometers) are less suited for quantitative determinations of fragment ion currents than systems with ordinary slit geometry.

Figure 4b shows the dependence of K on the kinetic energy as given by eqns. 1 and 2. This dependence may be used to correct measured fragment ion currents if the kinetic energy of the fragment ions is known (see below). Because of practical reasons (using the summation method for calibration of partial ionization cross-sections [18]) it is sufficient to normalize fragment ion currents to the efficiency of the thermal parent ion. Therefore we have also given in Fig. 4b the discrimination factor $D = K\ (E_{kin} = \text{thermal})/K(E_{kin})$ which allows correction of fragment ion currents to the same extraction efficiency as the parent ion. After such a correction all ion currents—fragment and parent—may be summed to total ion currents and calibrated against known total ionization cross-section values [18].

ION BEAM PROFILES AND INITIAL KINETIC ENERGY

Ion beam profile in the y*-direction*

Above we have derived a correction function ($D = D(E_{kin})$) which allows one to account for discrimination effects as a function of the initial kinetic energy. In order to apply this correction procedure the respective kinetic energies of the fragment ions under study must be known. In the following we will suggest a simple method using the same experimental set-up as described above to determine these properties.

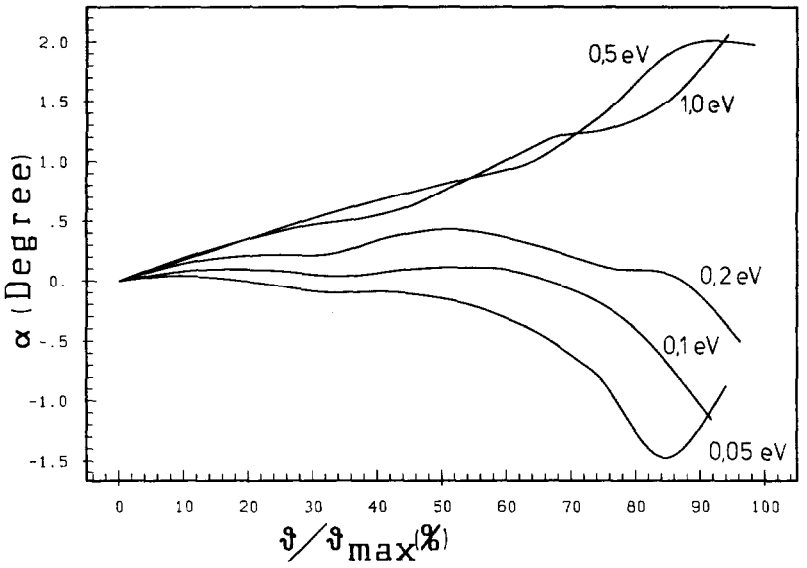

Fig. 5. Deflection angle α as a function of the reduced starting angle $\vartheta/\vartheta_{max}$ for different initial energies of the ions (for positive starting angles ϑ).

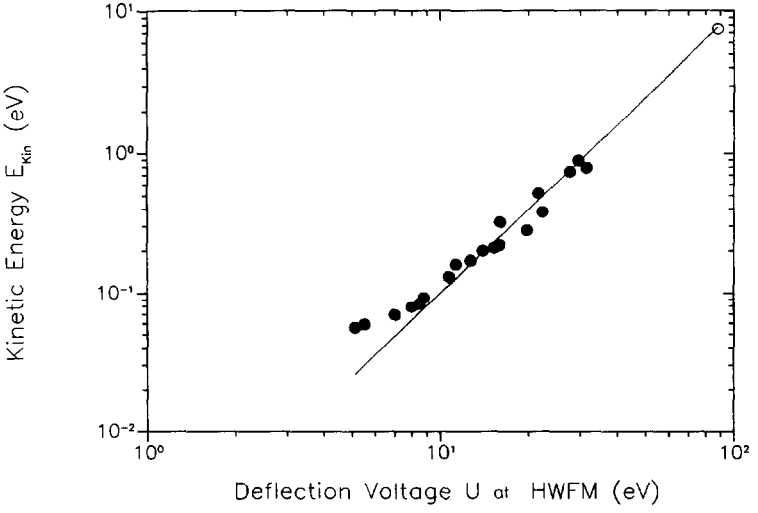

Fig. 6. Average kinetic energy of fragment ions (as reported by previous authors [11,20] versus z deflection voltage at HWFM (of the ion beam profile): (○), H^+ from H_2 corresponding to the high energy satellite peak [20]; (●), fragment ions from C_3H_8 (thermal and quasi-thermal peaks [11]); (——), calculated regression (see text) yielding a relationship $E_{kin} = 10^{-3} U^2$.

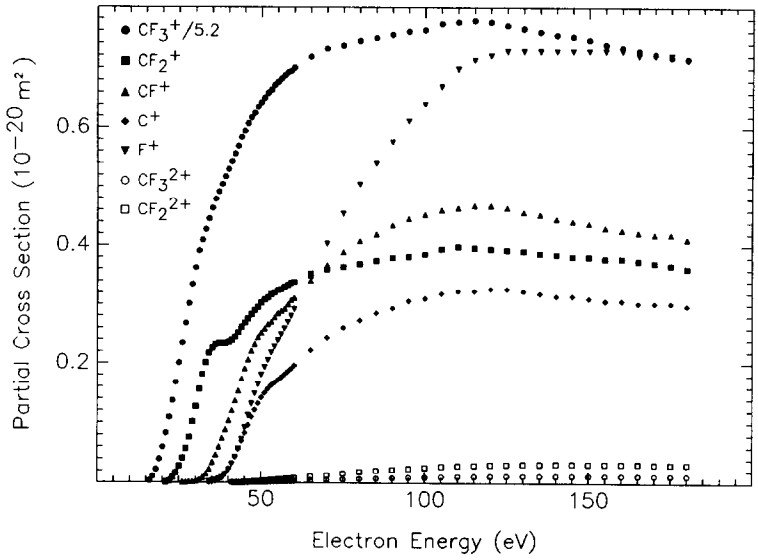

Fig. 7. Absolute partial electron impact ionization cross-sections vs. electron energy for fragment ions of CF_4 (present results).

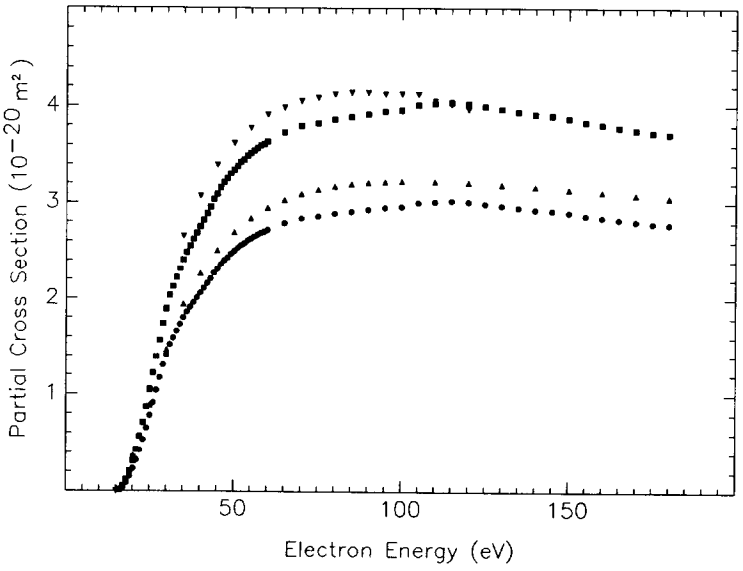

Fig. 8. Absolute cross-sections vs. electron energy for the production of CF_3^+ via $CF_4 + e \rightarrow CF_3^+$: (●), Stephan et al. 1985 [6] (uncorrected for kinetic energy effects); (▼), Poll and Meichsner 1987 [7]; (▲), Bonham and co-workers 1991 [23b]; (■), present results (data of ref. 6 corrected for kinetic energy effects).

Ion trajectory calculations in the x-y plane carried out for the ion paths beyond L_3 and L_4 show a complex behaviour (i.e. several cross-overs) depending strongly on the kinetic energy and leading to broad ion beam profiles in the y direction at the mass spectrometer entrance slit S_1 (as already mentioned and studied earlier [8,13–15]). This distribution of ions in front of S_1 may be measured experimentally (for details see refs. 8 and 14) by sweeping the ion beam across the mass spectrometer entrance slit with help of the deflection plates L_8 and L_9. To deflect the ion beam by an angle α (that is to move ions, which hit the mass spectrometer entrance slit plates under an angle α, to the axis of the ion optical system) a deflection voltage U is required across the deflector plates given by

$$U = \frac{2a}{l} \cdot U_B \cdot \tan \alpha \tag{3}$$

where a is the distance between L_8 and L_9, l is the length of the plates in the x direction and U_B is the ion acceleration voltage. Using the typical values of the CH5 mass spectrometer system ($a = 15\,\text{mm}$, $l = 21\,\text{mm}$, $U_B = 3\,\text{kV}$) gives $U \simeq 75\alpha$. The deflection angle α is directly related to the starting angle ϑ and the initial kinetic energy E_{kin} via the specific ion trajectory. It is possible to derive this relationship, $\alpha = \alpha(\vartheta, E_{kin})$, with the help of SIMION to give the desired link between the initial conditions of the ions and the ion beam profile in the y direction at S_1. Figure 5 shows α vs. ϑ (in reduced units $\vartheta/\vartheta_{max}$) for ions with different kinetic energies. It can be seen, however, that ion beam profiles constructed with the help of this relationship are not uniquely correlated to a specific energy. This is caused by vastly differing ion trajectories (focussing, cross-overs) for ions with different energies. It has to be concluded therefore that ion beam profiles obtained by scanning in the y direction cannot be used to deduce information on the kinetic energy[a]. The initial information regarding the kinetic energies is lost by the focussing action of the ion optical system.

Ion beam profile in the z direction

In contrast to the above mentioned case, ion motion in the z direction is influenced much less by the ion optical properties of the extraction and acceleration electrodes. Sen Sharma and Franklin [19] have demonstrated that z ion beam deflection profiles (see also earlier references given in ref. 19) may be used to measure the translational energies of fragment ions in good

[a] This is especially true in the case of fragment ions which are produced by different ionization channels leading to groups of fragment ions with well defined but widely differing excess kinetic energies. For instance CH_3^+ ions produced by electron impact ionization of C_3H_8 are generated with thermal energies and with energies of $\approx 1.44\,\text{eV}$ and $\approx 2.2\,\text{eV}$ [12].

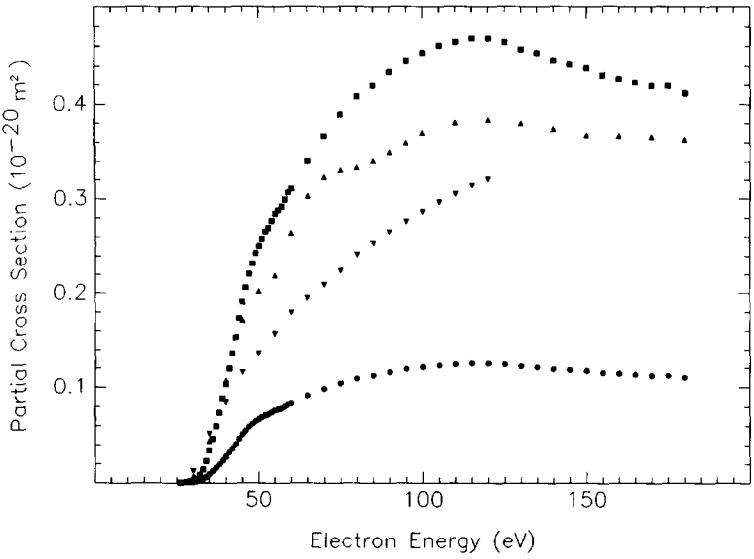

Fig. 9. Absolute cross-sections vs. electron energy for production of CF^+ via $CF_4 + e \rightarrow CF^+$: (●), Stephan et al. 1985 [6] (uncorrected for kinetic energy effects); (▼), Poll and Meichsner 1987 [7]; (▲), Bonham and co-workers 1991 [23b]; (■), present results (data of ref. 6 corrected for kinetic energy effects).

agreement with other methods. It can be shown easily (see eqn. 9 in ref. 19) that for a particular instrument the initial kinetic energy of an ion passing S_1 is proportional to the square of the deflection voltage. Moreover, for ions with thermal or quasi-thermal energy distributions the average translational energy of the fragment ions may be determined approximately from the half width at full maximum (HWFM) of the ion beam profile.

Following this approach we have plotted in Fig. 6 kinetic energies of fragment ions from H_2 and C_3H_8 determined previously by Köllmann [21] and by Fuchs and Taubert [11] respectively, versus the z deflection voltage determined at HWFM. It can be seen that most of the points lie close to the regression line, which we calculated using the relationship $E_{kin} \sim U_z^2$ (the deviation at almost thermal energy is due to different ion source temperatures in the experiment of Fuchs and Taubert and in the present case). It is of particular interest that not only quasi-thermal ions but also ions with rather large energies lie on this regression line. Moreover, it is also possible to analyze fragment ions which consist of more than one group of ions (e.g. the measured z profile of H^+ from H_2 can be interpreted in terms of at least two sets of ions, the high energy satellite peak corresponding to an average energy of ≈ 8 eV being in excellent agreement with all of the previous measurements [20]. It is therefore concluded that this method may be used in order to

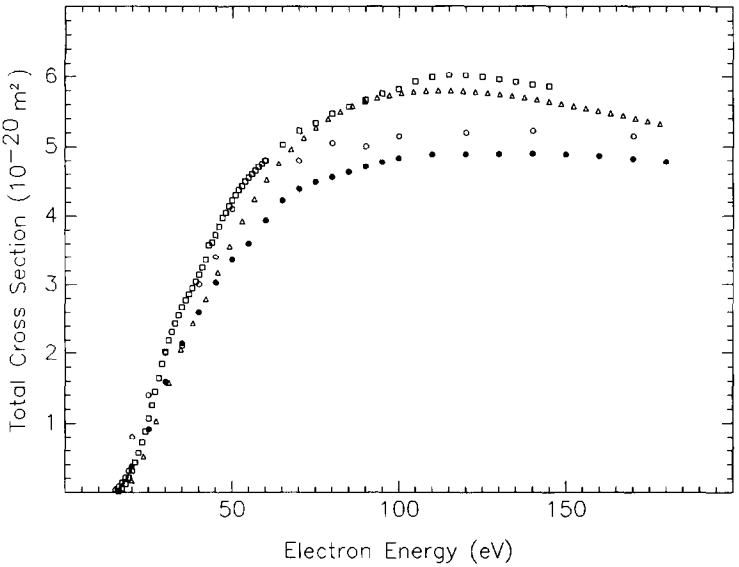

Fig. 10. Absolute total electron impact ionization cross-section function for CF_4: (□), present results (experimental data of ref. 6 corrected for kinetic energy effects); (△), calculated data using the semiclassical MDM approach [28,29]; (●), Bonham and co-workers 1991 [23b]; (○), Nishimura 1991 [26].

determine the initial kinetic energy necessary for use of the correction procedure outlined above.

ELECTRON IMPACT IONIZATION CROSS-SECTIONS FOR CF_4

Owing to the experimental difficulties outlined in the Introduction virtually no reliable partial ionization cross-sections for energetic fragment ions have been available in the literature for comparison (this has been discussed in detail in several recent reviews, see, e.g. refs. 1 and 2). Recently, several groups have, however, designed new research instruments to help alleviate this situation. Freund and co-workers [21] constructed an apparatus where a fast neutral beam is prepared by charge transfer neutralization of a selected ion beam and applied this technique to measure dissociative ionization of SiF_3, SiF_2 and SiF. Krishnakumar and Srivastava [22] and Ma et al. [23a] selected a pulsed electron beam approach in order to allow the determination of ions with high translational kinetic energies. Whereas first measurements of these groups were dedicated to rare gas ions and to N_2 fragment ions, Bonham has pointed out to us (during the preparation of this paper) the existence of very recent data on CF_4 measured in their group with an advanced pulsed electron beam time-of-flight instrument [23b]. As Bonham has been kind enough to send us this data on CF_4 in advance of publication we have taken CF_4 as a test

case for the correction procedure developed in the present study. This is possible because we have measured previously [6] not only absolute partial and total ionization cross-sections for CF_4, but also y and z ion beam profiles for all of the fragment ions of CF_4 using the same apparatus and experimental conditions as described in the present study.

Table 2 gives the z deflection U_z at HWFM for singly and doubly charged fragment ions of CF_4 taken from the z ion beam profiles given in ref. 6. Also shown are the corresponding average energies and discrimination factors as deduced from the relationships given in Figs. 6 and 4 respectively. Using these discrimination factors (which are, as expected, largest for the lighter fragment ions possessing higher dissociative kinetic energies) it is possible to correct the partial ionization cross-sections given in ref. 6. In Table 2 present results (at an energy of 80 eV) are compared with those from Bonham and co-workers [23b] and photo-ionization results obtained from an electron–ion coincidence experiment [24]. It is quite noteworthy that the relative abundances of singly charged fragment ions as obtained here by correcting our previous data [6] and from the two other studies are in excellent agreement. Moreover, Bonham and co-workers [23b] have determined relative cross-section ratios at 50, 75,

TABLE 2

Deflection voltage U_z at HWFM (from ref. 6), average kinetic energy E_{kin} (from Fig. 6), discrimination factor D (from Fig. 4) and percentage of the number of fragment ions at 80 eV electron energy P for CF_4. P (SDM) are data uncorrected for translational kinetic energy effects [6], P (present) are the presently corrected results, from SDM [6], P (MBB) are high accuracy results from ref. 23b and P (Aarts) are photoionization results obtained from an electron ion coincidence experiment [24]

Ion	U_z(V)	E_{kin} (eV)	D	P (SDM)	P (present)	P (MBB)	P (Aarts)
CF_3^+	8.1[a]	0.078[a]	1.34	86	70.6	70.6	67.3
CF_2^+	14.1	0.20	1.81	6.1	6.7	6.9	6.4
CF^+	25.6	0.63	3.74	3.2	7.5	7.4	6.5
F^+	38.7	1.41	7.20	2.1	9.2	8.1	12.5
C^+	28.1	0.75	4.19	1.9	5.0	5.4	6.2
CF_3^{2+}	6.2	0.053	1.04	0.2	0.1	0.5	-
CF_2^{2+}	6.9	0.060	1.16	0.5	0.3	1.0	1.1

[a] As compared with other fragment ions (including also other gases) the CF_3^+ ion exhibits a rather unusual z ion beam profile, i.e. consisting of a bimodular distribution. Here we have only considered one of the peaks. Both peaks taken together would correspond to an average kinetic energy of 0.26 eV, which is still much lower than the energy determined by Bonham and co-workers [23b] amounting to 1.5 ± 0.5 eV. At the moment we have no explanation for this discrepancy. If CF_3^+ ions do indeed have this high kinetic energy, a much larger correction factor D would be necessary. This in turn would drastically change the present cross-section of CF_3^+ and thus the total cross-section.

TABLE 3

Partial and total absolute electron impact ionization cross-sections for CF_4 (10^{-20} m^2). The present values have been obtained by correcting the data given in ref. 6 for translational kinetic energy discrimination effects

E(eV)	CF_3^+	CF_2^+	CF^+	C^+	F^+	CF_3^{2+}	CF_2^{2+}	q_{tot}
16	0.015							0.015
18	0.016							0.016
20	0.309							0.309
25	1.043	0.028						1.071
30	1.886	0.127	0.002					2.015
35	2.408	0.226	0.034		0.002			2.671
40	2.756	0.235	0.103	0.023	0.021			3.139
45	3.090	0.268	0.191	0.083	0.091			3.724
50	3.344	0.302	0.251	0.141	0.18		0.002	4.225
55	3.518	0.324	0.284	0.171	0.238	0.002	0.005	4.548
60	3.638	0.338	0.311	0.196	0.292	0.003	0.007	4.794
65	3.732	0.349	0.341	0.222	0.353	0.004	0.010	5.024
70	3.799	0.360	0.367	0.243	0.403	0.005	0.022	5.227
75	3.826	0.364	0.389	0.260	0.454	0.006	0.016	5.335
80	3.866	0.369	0.408	0.273	0.504	0.007	0.018	5.469
85	3.893	0.375	0.419	0.285	0.540	0.007	0.020	5.567
90	3.919	3.380	0.434	0.294	0.576	0.008	0.022	5.664
95	3.946	0.382	0.445	0.306	0.612	0.009	0.024	5.757
100	3.959	0.386	0.453	0.310	0.641	0.009	0.026	5.819
110	4.026	0.398	0.464	0.323	0.698	0.010	0.029	5.985
120	4.026	0.395	0.468	0.327	0.720	0.011	0.031	6.019
130	3.973	0.391	0.457	0.323	0.727	0.011	0.032	5.956
140	3.919	0.386	0.445	0.315	0.727	0.012	0.032	5.879
150	3.878	0.382	0.438	0.310	0.727	0.012	0.032	5.823
160	3.811	0.378	0.427	0.306	0.727	0.012	0.032	5.737
170	3.758	0.371	0.419	0.302	0.720	0.012	0.031	5.656
180	3.718	0.362	0.412	0.298	0.713	0.012	0.032	5.591

100, 130 and 180 eV for the two sets of measurements and found that the agreement between our corrected results and their results are all within the $\pm 15\%$ uncertainty assigned to each experiment. This demonstrates the usefulness of the present correction procedure to help alleviate discrimination effects in standard mass spectrometers. It is worth noting that the sum of the produced ions weighted with the corrected partial ionization cross-sections has a composition of $CF_{2.7}$. Thus, the stoichiometry has not changed much taking into account the discrimination effects due to initial kinetic energy. It has to be concluded, therefore, that the change in stoichiometry during the ionization process is as a result of factors inherent to the ionization processes. In general, the relative abundance of any fragment ion is related to its rate of formation and its rate of decomposition [25]. There are, however, several factors that will influence these rates, including the ionization energy. Moreover, according to Stevenson's rule in dissociative ionization of a molecule AB into A and B, the charge is preferentially retained at the fragment with the lower ionization energy [25].

It is also interesting to compare the corrected absolute ionization cross-sections (given in Table 3 and Fig. 7) with previous data. As two characteristic examples the results for CF_3^+ and CF^+ from refs. 6 and 7 (both uncorrected for ion translational energy) are compared in Figs. 8 and 9 with the corrected values of ref. 6, and the values from Bonham and co-workers [23b]. Despite the additional problem of the determination of the absolute scale in both experimental methods, satisfactory agreement exists between our corrected values and the data of Bonham and co-workers [23b]. Moreover, there exists excellent agreement (see Fig. 10) between the present total ionization cross-section, the total cross-sections of Bonham and co-workers [23b], and recent data obtained by Nishimura [26] using an apparatus described by Rapp and Englander-Golden [27]. All three sets of measurement are in addition in excellent agreement with predictions of a new semiclassical theory (MDM theory [28]) for calculating total ionization cross-sections for molecules [29].

Finally, it is important to note that there exists a serious disagreement for the doubly charged species. Cross-section ratios as well as absolute cross-sections are much smaller in our measurements than in the study of Bonham and co-workers [23b]. A similar disagreement with multiply charged species was also encountered in the case of studies on Ar between our group [14] and the group of Wetzel et al. [30] on the one hand and the data of Bonham and co-workers [23b] and Krishnakumar and Srivastava [22a] on the other hand (see also Fig. 1 in ref. 31). This important problem has been addressed recently in two studies [32,33]; the reasons for these discrepancies have, however, not revealed themselves as a result of these studies. Experiments in different laboratories are currently underway to provide the answer to this mystery.

ACKNOWLEDGEMENTS

This work was partially supported by the Österreichischer Fonds zur Förderung der Wissenschaftlichen Forschung and by the Bundesministerium für Wissenschaft und Forschung, Wien. We wish to thank Professor R.A. Bonham for sharing his ideas and latest results with us in advance of publication.

REFERENCES

1 T.D. Märk, in L.G. Christophorou (Ed.), Electron Molecule Interactions and their Applications, Vol. 1, Academic Press, Orlando, FL, 1984, p. 251; I.A.E.A. Tech. Doc., 506 (1989) 179.
2 T.D. Märk and G.H. Dunn, Electron Impact Ionization, Springer-Verlag, Vienna, 1985.
3 L.C. Pitchford, B.V. McKoy, A. Chutjian and S. Trajmar (Eds.), Swarm Studies and Inelastic Electron–Molecule Collisions, Springer-Verlag, New York, 1987, pp. 369–423.
4 T. Stanski and A. Adamczyk, Int. J. Mass Spectrom. Ion Phys., 46 (1983) 31.
5 K. Leiter, K. Stephan, E. Märk and T.D. Märk, Plasma Chem. Plasma Processes, 4 (1984) 235.
6 K. Stephan, H. Deutsch and T.D. Märk, J. Chem. Phys., 83 (1985) 5712.
7 H.U. Poll and J. Meichsner, Contrib. Plasma Phys., 27 (1987) 359.
8 K. Leiter, P. Scheier, G. Walder and T.D. Märk, Int. J. Mass Spectrom. Ion Processes, 87 (1989) 209.
9 J.P. Johnson and J.L. Franklin, Int. J. Mass Spectrom. Ion Phys., 33 (1980) 393.
10 J. Olmsted III, K. Street, Jr. and A.S. Newton, J. Chem. Phys., 40 (1964) 2114.
11 R. Taubert, Z. Naturforsch., Teil A, 19 (1964) 484, 911; R. Fuchs and R. Taubert, Z. Naturforsch., Teil A, 19 (1964) 494, 1181; 20 (1965) 823.
12 A.I. Ossinger and E.R. Weiner, J. Chem. Phys., 65 (1976) 2892.
13 T.D. Märk, Beitr. Plasmaphys., 22 (1982) 257.
14 K. Stephan, H. Helm and T.D. Märk, J. Chem. Phys., 73 (1980) 3763.
15 T.D. Märk, P. Scheier, K. Leiter, W. Ritter, K. Stephan and A. Stamatovic, Int. J. Mass Spectrom. Ion Processes, 74 (1986) 281.
16 SIMION, Version 3.0, Idaho National Engineering Laboratory, EG & G Idaho Inc., Idaho Falls, ID, 1987.
17 H.W. Werner, Int. J. Mass Spectrom. Ion Phys., 14 (1974) 189.
18 T.D. Märk, in T.D. Märk and G.H. Dunn (Eds.), Electron Impact Ionization, Springer-Verlag, Vienna, 1985, Chapter 5.
19 D.K. Sen Sharma and J.L. Franklin, Int. J. Mass Spectrom. Ion Phys., 13 (1974) 139.
20 K. Köllmann, Int. J. Mass Spectrom. Ion Phys., 17 (1975) 261.
21 T.R. Hayes, R.C. Wetzel, F.A. Baiocchi and R.S. Freund, J. Chem. Phys., 88 (1988) 823. R.S. Shul, T.R. Hayes, R.C. Wetzel, F.A. Baiocchi and R.S. Freund, J. Chem. Phys., 89 (1988) 4042.
T.R. Hayes, R.J. Schul, F.A. Baiocchi, R.C. Wetzel and R.S. Freund, J. Chem. Phys., 89 (1988) 4035.
22 E. Krishnakumar and S.K. Srivastava, J. Phys. B, (a) 21 (1988) 1055; (b) 23 (1990) 1893.
23 C. Ma, C.H. Sporleder and R.A. Bonham, (a) Rev. Sci. Instrum., 62 (1991) 909; (b) Phys. Rev. A, 44 (1991) 2921.
24 J.F.M. Aarts, Chem. Phys. Lett., 114 (1985) 114.

25 T.D. Märk, in L.G. Christophorou (Ed.), Electron–Molecule Interactions and Their Applications, Academic Press, Orlando, FL, 1984, pp. 267, 268.
26 H. Nishimura, in K. Tachibana (Ed.), Proc. 8th Symp. Plasma Processing, Nagoya, Japan, pp. 333–336.
27 D. Rapp and P. Englander-Golden, J. Chem. Phys., 43 (1965) 1464.
28 D. Margreiter, H. Deutsch and T.D. Märk, Contrib. Plasma Phys., 30 (1990) 487.
29 D. Margreiter, H. Deutsch, H. Schmidt and T.D. Märk, Int. J. Mass Spectrom. Ion Processes, 100 (1990) 157.
30 R.C. Wetzel, F.A. Baiocchi, T.R. Hayes and R.S. Freund, Phys. Rev. A, 35 (1987) 559.
31 D. Margreiter, G. Walder, H. Deutsch, H.U. Poll, C. Winkler, K. Stephan and T.D. Märk, Int. J. Mass Spectrom. Ion Processes, 100 (1990) 143.
32 R.A. Bonham and M.R. Bruce, Commun. At. Mol. Phys., (1991) submitted.
33 V. Tarnovsky and K. Becker, Z. Phys. D, (1991) submitted.